



## Oblique Incidence Reflectivity Difference as an *In Situ* Probe of Co Electrodeposition on Polycrystalline Au

W. Schwarzacher,<sup>a,\*</sup> J. Gray,<sup>b</sup> and X. D. Zhu<sup>b</sup>

<sup>a</sup>H. H. Wills Physics Laboratory, Bristol BS8 1TL, United Kingdom

<sup>b</sup>Department of Physics, University of California, Davis, California 95616, USA

We apply a special form of ellipsometry, oblique incidence optical reflectivity difference (OI-RD), which is optimized to detect changes at a surface, to Co electrodeposition on polycrystalline Au. The OI-RD signal is shown to be proportional to Co thickness and thus enables the separation of the Co deposition and H<sub>2</sub> evolution partial currents. Competition between the two processes gives rise to interesting effects, including the observation of a peak in the Co partial current during both the anodic and cathodic sweeps of a cyclic voltammogram taken after repeated cycles of Co deposition and dissolution.

© 2003 The Electrochemical Society. [DOI: 10.1149/1.1562072] All rights reserved.

Manuscript submitted September 6, 2002; revised manuscript received January 14, 2003. Available electronically March 13, 2003.

When studying the early stages of metal electrodeposition, *in situ* techniques such as scanning tunneling microscopy (STM), X-ray diffraction (XRD), and the electrochemical quartz-crystal microbalance (EQCM) have proved valuable complements to electrochemical methods based on measuring the deposition current and potential. *In situ* optical methods ranging from Raman spectroscopy to ellipsometry have also made important contributions.<sup>1,2</sup> Here we describe a special form of ellipsometry, oblique incidence optical reflectivity difference (OI-RD), optimized to probe changes that take place at the surface of a substrate.<sup>3-7</sup>

Co electrodeposition is of particular interest because of its magnetic properties. Electrodeposited Co alloy/Cu multilayers have been shown to possess giant magnetoresistance (GMR),<sup>8</sup> while ultrathin electrodeposited Co films on Au(111) exhibit perpendicular magnetic anisotropy (PMA).<sup>9</sup>

In this work we demonstrate that for ultrathin Co films electrodeposited on polycrystalline Au, the OI-RD signal from the surface in response to the Co coverage may be used like the output of an EQCM to separate the contributions of hydrogen evolution and Co deposition to the cathodic current, and therefore provide insight into competition between these processes. The OI-RD technique has certain advantages over the EQCM for this purpose, for example, it provides information only from the region probed by the optical beam, whereas the EQCM averages over the whole sample. Because the OI-RD technique, unlike EQCM, does not require a special substrate, it could in principle be incorporated in production processes for measuring the thickness of electrodeposited films *in situ*. Co electrodeposition is a good example of a system where a precise measurement of this kind is important, because both GMR and PMA are highly sensitive to Co layer thickness.

### Experimental

Figure 1 shows the electrochemical cell and optical arrangement used here. The cell, which has dimensions 80 mm length × 14 mm width × 50 mm height, contains a saturated calomel reference electrode and a Pt counter electrode facing the working electrode (substrate). The latter was a polycrystalline Au film evaporated on a glass microscope slide with a Ti adhesion layer. Unless otherwise stated, the electrolyte was 1 mM CoSO<sub>4</sub> + 10 mM K<sub>2</sub>SO<sub>4</sub> + 0.1 mM KCl + 1 mM H<sub>2</sub>SO<sub>4</sub>,<sup>10</sup> deaerated by bubbling N<sub>2</sub> through it for at least 15 min. Co was deposited under potentiostatic control.

The working principles of the OI-RD have been described by Zhu and co-workers before.<sup>3-7</sup> The light source in our experiment is a 5 mW He-Ne laser. The laser beam polarization is modulated

between *p*- (electric field parallel to reflection plane) and *s*- (electric field perpendicular to reflection plane) at a frequency Ω = 50 kHz with a photoelastic modulator (Hinds Instruments PEM 90). The polarization-modulated beam enters and exits the electrochemical cell through quartz windows and is reflected from the sample at an incidence angle of θ<sub>i</sub> = 72.5°. The reflected laser intensity has terms that vary with time at various harmonics of the modulation frequency Ω. We measure the second harmonic, I(2Ω), with a lock-in amplifier. Let r<sub>p</sub> and r<sub>s</sub> be the sample reflectivity for *p*- and *s*-polarized light during electrodeposition. Let r<sub>p0</sub> and r<sub>s0</sub> be the corresponding values for the substrate. We define Δ<sub>p</sub> = (r<sub>p</sub> - r<sub>p0</sub>)/r<sub>p0</sub> and Δ<sub>s</sub> = (r<sub>s</sub> - r<sub>s0</sub>)/r<sub>s0</sub>. Prior to electrodeposition, we adjust the transmission axis of the analyzer so that I(2Ω) is close to zero. The subsequent change in I(2Ω) has been shown<sup>3-7</sup> to be proportional to the real part of Δ<sub>p</sub> - Δ<sub>s</sub>, namely, Re{Δ<sub>p</sub> - Δ<sub>s</sub>}. Experimentally we can determine the proportionality constant separately so that we obtain Re{Δ<sub>p</sub> - Δ<sub>s</sub>} directly. For films with thickness much less than the optical wavelength λ, Δ<sub>p</sub> - Δ<sub>s</sub> varies with the film thickness *d* and other properties of the surface as follows<sup>3</sup>

$$\Delta_p - \Delta_s = i \frac{4\pi d}{\lambda} \sqrt{\epsilon_a} \cos \theta_i \sin^2 \theta_i \times \frac{\epsilon_{\text{Au}}(\epsilon_a - \epsilon_{\text{Co}})(\epsilon_{\text{Co}} - \epsilon_{\text{Au}})}{\epsilon_{\text{Co}}(\epsilon_{\text{Au}}^2 \cos^2 \theta_i - \epsilon_a \epsilon_{\text{Au}} + \epsilon_a^2 \sin^2 \theta_i)} \quad [1]$$

Here ε<sub>a</sub> is the optical dielectric constant of the electrolyte at the He-Ne laser wavelength. ε<sub>Co</sub> and ε<sub>Au</sub> are the optical dielectric constants for the electrodeposited Co and the gold substrate, respectively. We used a computer-aided data acquisition system to collect the optical and electrochemical data simultaneously. Although the

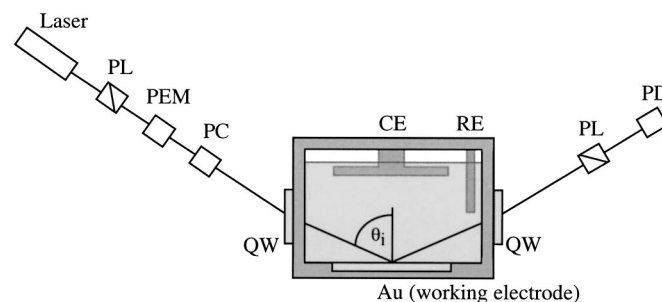


**Figure 1.** Experimental apparatus for the *in situ* OI-RD measurements. PL: Glan-Thompson polarizers; PEM: photoelastic modulator; PC: Pockels cell; QW: quartz window; CE: counter electrode; RE: reference electrode; PD: biased silicon photodiode.

\* Electrochemical Society Active Member.

<sup>z</sup> E-mail: w.schwarzacher@bristol.ac.uk

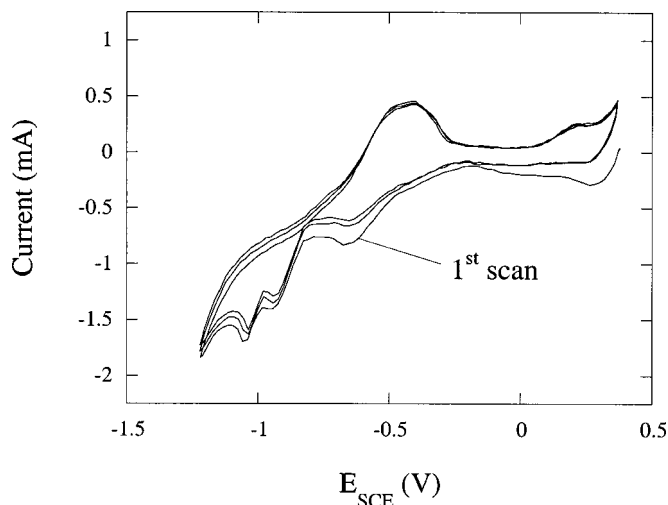


**Figure 2.** CV obtained from clean polycrystalline Au substrate and 1 mM CoSO<sub>4</sub> + 10 mM K<sub>2</sub>SO<sub>4</sub> + 0.1 mM KCl + 1 mM H<sub>2</sub>SO<sub>4</sub> electrolyte at 20 mV s<sup>-1</sup>.

work described here involves very dilute Co electrolytes, Co concentrations as high as 0.2 M are still sufficiently transparent to give a good signal-to-noise ratio for  $Re\{\Delta_p - \Delta_s\}$ .

### Results and Discussion

Figure 2 shows a typical cyclic voltammogram (CV) obtained with a scan rate of 20 mV s<sup>-1</sup>. It is similar to those reported by Cagnon *et al.*<sup>10</sup> The cathodic waves at  $E_{SCE} = -1.0$  V and  $-0.8$  V correspond to bulk Co deposition and proton reduction, respectively, while the anodic wave at  $E_{SCE} = -0.35$  V corresponds to Co oxidation and dissolution. Note that the proton reduction peak occurs at a more negative potential on the first scan. This is probably because on subsequent scans a small quantity of Co remains at the Au surface and lowers the hydrogen overpotential.

Figure 3 shows the results of a typical pulsed deposition experiment. The potential applied to the substrate ( $E_{SCE}$ ) is stepped from ( $E_{SCE} + 0.375$  V, which is positive of the Co dissolution potential, to  $-0.895$  V, at which both H<sub>2</sub> evolution and Co deposition take place, for  $\sim 130$  s, as shown in Fig. 3a. During this interval a cathodic current that decreases in magnitude is recorded, followed by an anodic current when the substrate potential returns to  $+0.375$  V and the Co dissolves, as shown in Fig. 3b. The optical signal  $Re\{\Delta_p - \Delta_s\}$  increases as Co is deposited, and returns to its initial value when the Co dissolves, as shown in Fig. 3c. The initial drop in  $Re\{\Delta_p - \Delta_s\}$  at  $t \sim 30$  s is most likely due to nonfaradaic processes. Changes in optical dielectric parameters of electrode surfaces due to such processes have previously been observed in double-layer regions.<sup>11</sup> To check that the change in  $Re\{\Delta_p - \Delta_s\}$  is proportional to the Co film thickness  $d$ , in Fig. 4 we plot the maximum change in  $Re\{\Delta_p - \Delta_s\}$  for a series of deposition experiments like that of Fig. 3, as a function of the integral  $\Delta Q$  of the anodic current recorded following the deposition pulse. We assume that  $\Delta Q$  is proportional to the quantity of Co deposited. As expected, the data fall on a straight line. The reason that this line does not pass through the origin is that  $\Delta Q$  presumably contains a contribution from discharge of the double layer. Since the charge per monolayer is 0.59 mC/cm<sup>2</sup>,<sup>10</sup> the measured change in  $Re\{\Delta_p - \Delta_s\}$  per monolayer of the deposited Co is 0.009. From Eq. 1 and

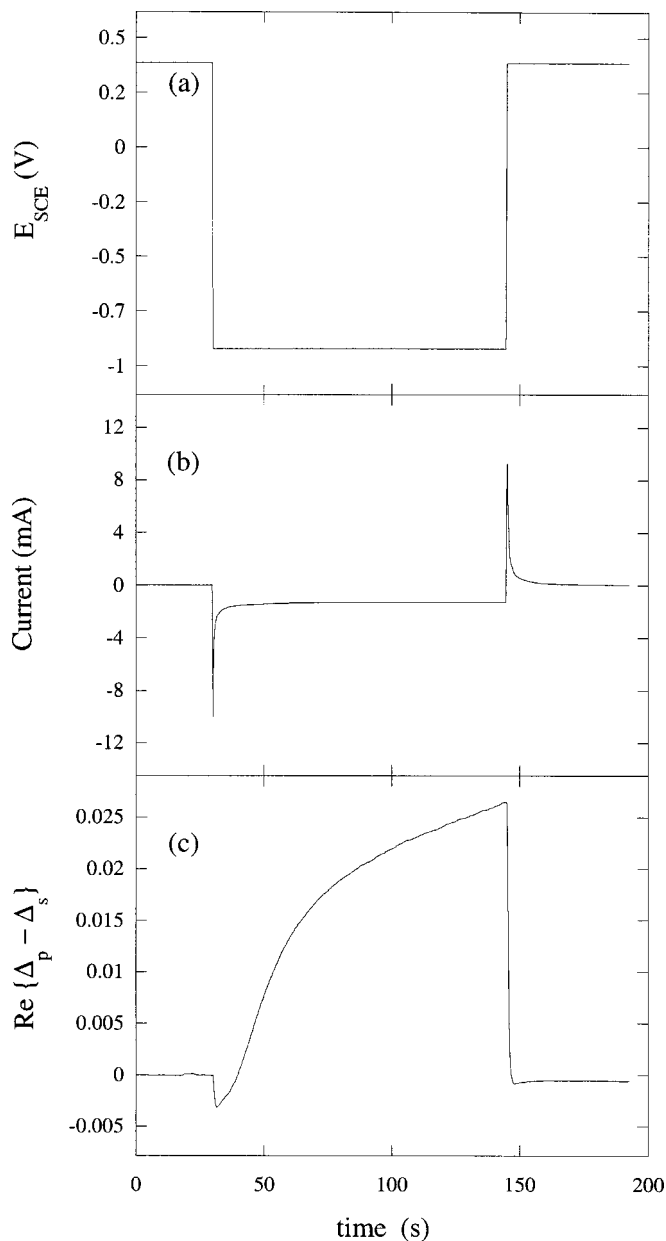


**Figure 3.** (a) Substrate potential, (b) current, and (c)  $Re\{\Delta_p - \Delta_s\}$  recorded during a typical Co deposition experiment.

using the bulk optical dielectric constants,  $\epsilon_a = 1.77$  for the solution that is essentially pure water,  $\epsilon_{Au} = -9.98 + i 0.85$ ,  $\epsilon_{Co} = -11.62 + i 18.47$ ,<sup>12</sup> we find that the calculated  $Re\{\Delta_p - \Delta_s\}$  is 0.01 for one smooth and compact monolayer Co with thickness  $d = 2.5$  Å on Au. The calculation and the experiment agree quantitatively.

Given that  $Re\{\Delta_p - \Delta_s\}$  is proportional to  $d$ , the optical signal may be used to separate the contribution of Co deposition and H<sub>2</sub> evolution to the cathodic current, and study the competition between these two processes. Figure 5 shows the optical signal  $Re\{\Delta_p - \Delta_s\}$  recorded during two different deposition experiments. In one, the potential was stepped directly from  $+0.375$  V to  $-0.895$  V, where H<sub>2</sub> evolution and Co deposition both take place, while in the second it was stepped from  $+0.375$  V to  $-0.795$  V, where only H<sub>2</sub> evolution occurs, for 83 s before a further step to  $-0.895$  V. In the figure,  $t = 0$  corresponds to the point at which the potential was switched to  $-0.895$  V.  $Re\{\Delta_p - \Delta_s\}$ , and therefore the amount of

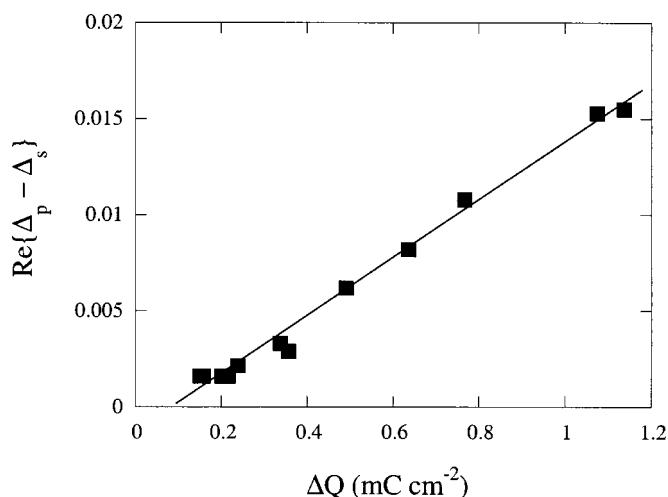


**Figure 4.** Maximum change in  $Re\{\Delta_p - \Delta_s\}$  as a function of the integral  $\Delta Q$  of the anodic current recorded following the deposition pulse in a series of experiments like that of Fig. 3.

deposited Co, rises much more rapidly at  $t = 0$  when the potential was previously at  $-0.795$  than  $+0.375$  V. This is easily explained by the competition between Co deposition and  $H_2$  evolution: if the potential is held at  $-0.795$  V, the region close to the substrate becomes depleted of protons, so Co deposition is favored over proton reduction when the potential is switched to  $-0.895$  V. This competition and the consequent variation of the Co current efficiency, is relevant to the electrodeposition of multilayers.<sup>13</sup>

When Co is repeatedly deposited and stripped from Au, the electrochemical response of the substrate changes, presumably because some quantity of Co remains at the surface, which may be seen by comparing Fig. 6, taken after several deposition/stripping experiments, with Fig. 2.

The optical signal can help in identifying features in the CV associated with Co deposition. Since  $Re\{\Delta_p - \Delta_s\}$  is proportional to the quantity of deposited Co (see Fig. 4), its time derivative,  $dRe\{\Delta_p - \Delta_s\}/dt$ , is then proportional to the Co partial current. In Fig. 7, the time derivative of  $Re\{\Delta_p - \Delta_s\}$ , the total current  $i$ , and the applied potential are plotted as a function of time for one cycle

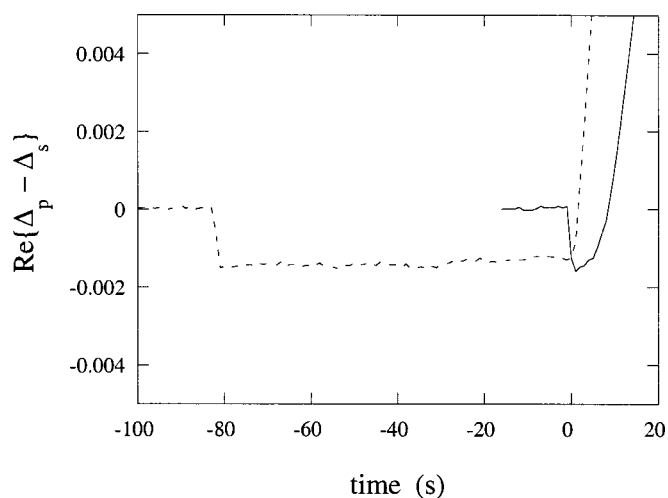


**Figure 5.**  $Re\{\Delta_p - \Delta_s\}$  recorded (---) when the substrate potential was stepped to  $-0.795$  V for 83 s prior to being stepped to  $-0.895$  V at  $t = 0$ , and (—) when the substrate potential was stepped directly from  $+0.375$  to  $-0.895$  V at  $t = 0$ .

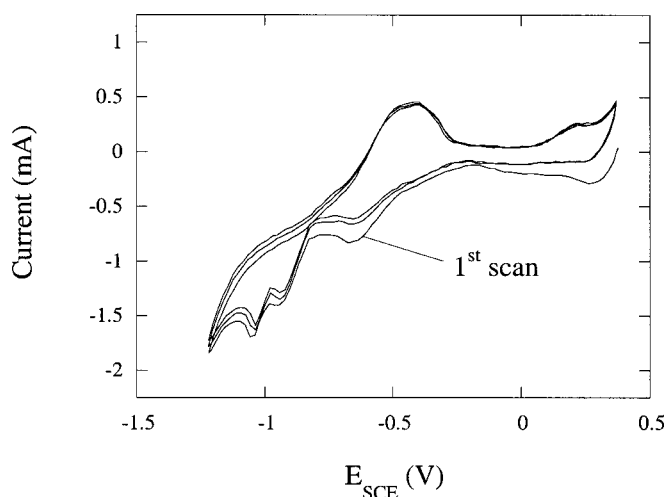


**Figure 6.** As for Fig. 2, but after some CV and deposition/dissolution experiments.

of the CV of Fig. 2. The derivative has been normalized so that its maximum positive value is equal to the maximum anodic current. Note how closely the derivative of  $Re\{\Delta_p - \Delta_s\}$  matches  $i$  around  $t \sim 120$  s and  $E_{SCE} \sim -0.35$  V, where Co stripping occurs, supporting the assumption that it is proportional to the Co partial current. There is no peak in the derivative of  $Re\{\Delta_p - \Delta_s\}$  corresponding to the first cathodic peak in  $i$  around  $t \sim 60$  s and  $E_{SCE} \sim -0.82$  V, indicating that this peak is due to  $H_2$  evolution (proton reduction).

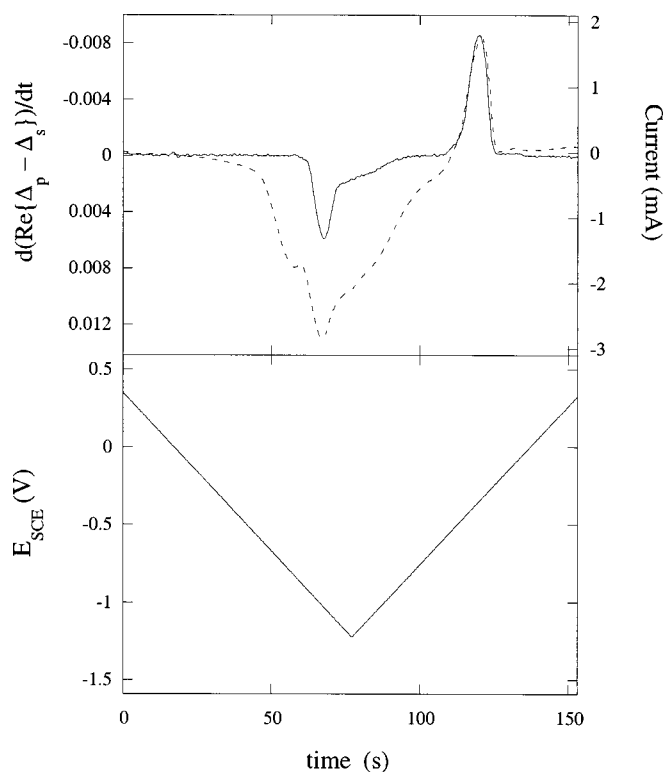


**Figure 7.** (—) The time derivative of  $Re\{\Delta_p - \Delta_s\}$ , (---) the total current, and (bottom) applied potential as a function of time for one cycle of the CV of Fig. 2.

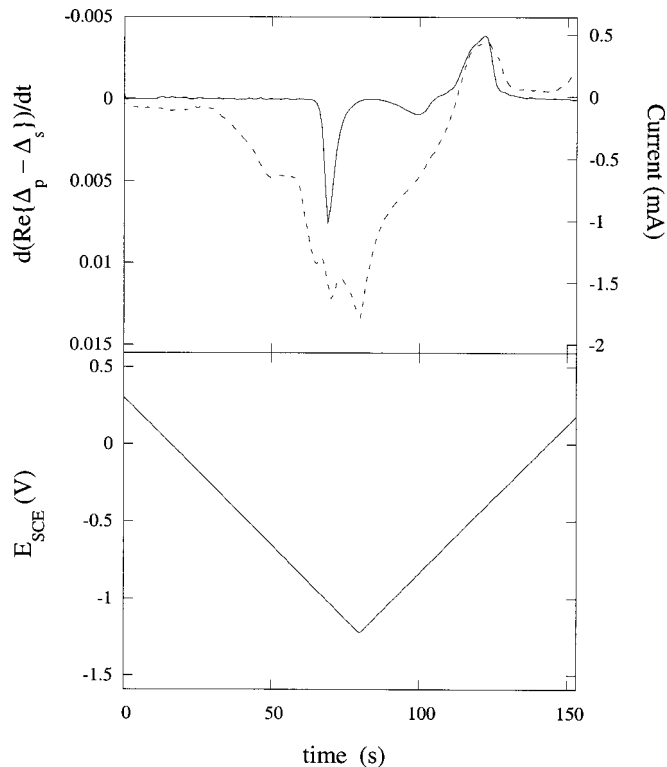


**Figure 8.** (—) The time derivative of  $Re\{\Delta_p - \Delta_s\}$ , (----) the total current, and (bottom) applied potential as a function of time for one cycle of the CV of Fig. 6.

Figure 8 shows  $d Re\{\Delta_p - \Delta_s\}/dt$ , the total current  $i$ , and the applied potential as a function of time for one cycle of the CV of Fig. 6. It is clear that neither of the two cathodic peaks in  $i$  around  $t \sim 50$  s and  $E_{SCE} \sim -0.65$  V and  $t \sim 65$  s and  $E_{SCE} \sim -0.95$  V are associated with Co deposition. Possibly they are associated with proton reduction at different sites, with the first peak being associated with  $H_2$  evolution at regions of the surface where Co remains after the preceding deposition/stripping experiments. An interesting feature of this data is that there is a second peak in  $d Re\{\Delta_p - \Delta_s\}/dt$  corresponding to Co deposition at  $t \sim 95$  s and

$E_{SCE} \sim -0.85$  V. There is a peak in the Co partial current during both the anodic and the cathodic sweeps of the CV. This again demonstrates the competition between  $H_2$  evolution and Co deposition: during the cathodic sweep, Co depletion and the onset of  $H_2O$  electrolysis suppress Co deposition, but as the potential is swept in the positive direction, the rate of  $H_2O$  electrolysis decreases and allows Co deposition to increase.

To conclude, we have demonstrated that the OI-RD measured during electrodeposition of one metal on another is proportional to the overlayer thickness. Consequently, this technique provides a useful alternative to the EQCM. For the Co on Au system studied, the technique revealed details of the competition between Co deposition and  $H_2$  evolution.

### Acknowledgments

W.S. thanks the U.S.-U.K. Fulbright Commission for a scholarship, C. and N. Foster, and the National Institute of Standards and Technology for their hospitality. X.D.Z. acknowledges the support of this work by the U.S. National Science Foundation under grant no. DMR-9818483.

University of California, Davis, assisted in meeting the publication costs of this article.

### References

1. D. M. Kolb, in *Spectroelectrochemistry: Theory and Practice*, R. J. Gale, Editor, p. 87, Plenum Press, New York (1988).
2. R. H. Muller, in *Advances in Electrochemistry and Electrochemical Engineering*, Vol. 9, R. H. Muller, Editor, p. 167, Wiley, New York (1973).
3. A. Wong and X. D. Zhu, *Appl. Phys. A: Mater. Sci. Process.*, **63**, 1 (1996).
4. X. D. Zhu, H. B. Lu, G. Z. Yang, Z. Y. Li, B. Y. Gu, and D. Z. Zhang, *Phys. Rev. B*, **57**, 2514 (1998).
5. X. D. Zhu, W. Si, X. X. Xi, Q. Li, and M. G. Medici, *Appl. Phys. Lett.*, **74**, 3540 (1999).
6. X. D. Zhu, W. Si, X. X. Xi, and Q. D. Jiang, *Appl. Phys. Lett.*, **78**, 460 (2001).
7. F. Chen, T. Zhao, Y. Y. Fei, H. B. Lu, Z. H. Chen, G. Z. Yang, and X. D. Zhu, *Appl. Phys. Lett.*, **80**, 2889 (2002).
8. W. Schwarzacher and D. S. Lashmore, *IEEE Trans. Magn.*, **32**, 3133 (1996).
9. J. L. Bubendorff, E. Beaurepaire, C. Mény, P. Panissod, and J. P. Bucher, *Phys. Rev. B*, **56**, R7120 (1997).
10. L. Cagnon, T. Devolder, R. Cortes, A. Morrone, J. E. Schmidt, C. Chappert, and P. Allongue, *Phys. Rev. B*, **63**, 104419 (2001); L. Cagnon, A. Gündel, T. Devolder, A. Morrone, C. Chappert, J. E. Schmidt, and P. Allongue, *Appl. Surf. Sci.*, **164**, 22 (2000).
11. M. Stedman, *Chem. Phys. Lett.*, **2**, 457 (1968).
12. J. H. Weaver and D. W. Lynch, *Optical Properties of Metals 18*, no. 2, Fachinformationszentrum, Karlsruhe (1981).
13. A. Gündel, E. Chassaing, and J. E. Schmidt, *J. Appl. Phys.*, **90**, 5257 (2001).